

## Search for particle-bound $^{26}\text{O}$ and $^{28}\text{F}$ in $p$ -stripping reactions

A. Schiller,<sup>1,\*</sup> T. Baumann,<sup>1</sup> J. Dietrich,<sup>1,†</sup> S. Kaiser,<sup>1,†</sup> W. Peters,<sup>1,2</sup> and M. Thoennessen<sup>1,2</sup>

<sup>1</sup>National Superconducting Cyclotron Laboratory, Michigan State University, East Lansing, Michigan 48824, USA

<sup>2</sup>Michigan State University, Department of Physics and Astronomy, East Lansing, Michigan 48824, USA

(Received 5 April 2005; published 15 September 2005)

We have searched for particle-bound  $^{26}\text{O}$  and  $^{28}\text{F}$  isotopes in the reaction products of secondary  $^{27}\text{F}$  and  $^{29}\text{Ne}$  beams, respectively. No events have been observed. Upper limits of 3.3 mb and 1.2 mb for the respective production cross sections of  $^{26}\text{O}$  and  $^{28}\text{F}$  by one  $p$ -stripping reactions are established. Since in the case of  $^{28}\text{F}$ , this upper limit is sufficiently small compared to common estimates, we conclude that  $^{28}\text{F}$  is most likely unbound. For the case of  $^{26}\text{O}$ , our result is not statistically significant, thus, the question cannot be answered whether  $^{26}\text{O}$  is a particle-unbound nucleus or not.

DOI: [10.1103/PhysRevC.72.037601](https://doi.org/10.1103/PhysRevC.72.037601)

PACS number(s): 21.10.Dr, 25.60.Dz, 27.30.+t

The existence of particle-bound isotopes with given numbers of protons and neutrons is one of the most fundamental questions in nuclear physics. Particularly intriguing is the fact that in projectile fragmentation reactions oxygen isotopes have been found only for neutron numbers up to  $N = 16$  [1] while neighboring fluorine isotopes can be found to up to at least  $N = 22$  [2]. This means that one proton in the  $sd$  shell can bind as many as six more neutrons beyond the new magic number  $N = 16$  [3]. Although modern theory with new effective interactions has been successful in explaining this observation in terms of the effective single-particle energy of the  $\nu 0d_{3/2}$  orbital [3] and how this energy is modified by the presence of one or more protons in the  $\sigma\tau$ -partner orbital  $\pi 0d_{5/2}$  [4,5], one question remains. Since theory predicts  $^{26}\text{O}$  to be particle unbound by only about 20 keV [3,6] and production cross sections in projectile fragmentation reactions decrease sharply with decreasing particle-separation energy of the desired reaction product [7,8], there remains a possibility for  $^{26}\text{O}$  to be marginally bound and thus observable only in less violent types of reactions for which production cross sections do not depend strongly on particle-separation energies.

For this reason, we have investigated the  $p$ -stripping reaction of a radioactive  $^{27}\text{F}$  beam on a 146-mg/cm<sup>2</sup>-thick carbon target at beam energies of  $\sim 90$  MeV/nucleon. The experiment was performed at the Coupled Cyclotron Facility of the National Superconducting Cyclotron Laboratory at Michigan State University. A 142 MeV/nucleon  $^{48}\text{Ca}$  beam was fragmented on an 846-mg/cm<sup>2</sup>-thick Be target. Reaction products from this target were selected using the A1900 fragment separator with a 971-mg/cm<sup>2</sup>-thick acrylic wedge at the intermediate image. The momentum acceptance was limited to 1%. Major impurities with roughly equal intensities as the desired  $^{27}\text{F}$  beam were  $^{29}\text{Ne}$  and  $^{30}\text{Na}$ . The presence of  $^{29}\text{Ne}$  in the beam enabled us to also investigate the  $p$ -stripping reaction from this nucleus and to address the question whether  $^{28}\text{F}$  can be observed among the reaction products or not. The

total number of incoming beam particles was  $3 \times 10^5$  and  $5 \times 10^5$  for  $^{27}\text{F}$  and  $^{29}\text{Ne}$ , respectively.

At the focus of the fragment separator, a stack of Si detectors was mounted which also contained the secondary carbon reaction target (see Fig. 1). The stack consisted of a 100- $\mu\text{m}$ -thick Si surface-barrier detector (#0) to identify the incoming beam particles event by event using the energy-loss time-of-flight technique, the secondary reaction target, two more 100- $\mu\text{m}$ -thick Si surface-barrier detectors (#1,2), three 5000- $\mu\text{m}$ -thick Li-drifted Si detectors (#3–5), and a scintillation veto detector. The oxygen and fluorine reaction products of interest are stopped in the final Si detector (#5). Light charged particles like, e.g., protons from diffraction-dissociation events will make it into the plastic scintillation detector. The setup is nearly identical to the setup in a previous experiment for measuring one- $p$ -stripping cross sections from  $^{24-26}\text{F}$  [9].

The Si detectors were calibrated using  $^{19-22}\text{O}$  and  $^{21-25}\text{F}$  isotopes of several known energies, beams of which were created in runs of the A1900 fragment separator with different  $B\rho$  settings and without the acrylic wedge. These beams were also used to calibrate the mass-indicator spectra which are used to separate different isotopes created in the stripping reactions. In the data analysis, particles of interest were identified by their large energy deposition in the three thick detectors (#3–5). Unreacted beam particles were separated from lower- $Z$  reaction products by the somewhat smaller energy deposition of the latter in the first three detectors behind the target (#1–3). The detailed pattern of energy deposition in the three thick detectors (#3–5) was used to construct three different mass indicators of which the first two do not rely on any specific functional form of the range curve. Range curves, i.e., penetration depths as function of kinetic energy  $R(E)$  are calculated for  $^{26}\text{O}$  and  $^{28}\text{F}$  in silicon and fitted by third-order polynomials. So-called thickness spectra can then serve as mass indicators. In our case, we used

$$t_{3,4} = R(E_{\#3} + E_{\#4} + E_{\#5}) - R(E_{\#5}), \quad (1)$$

$$t_4 = R(E_{\#4} + E_{\#5}) - R(E_{\#5}), \quad (2)$$

which for the desired isotopes yield the correct thicknesses of the Si detectors #3 + #4 and #4 for  $t_{3,4}$  and  $t_4$ , respectively. Lighter isotopes of the same element yield smaller “effective”

\*Electronic address: schiller@nscl.msu.edu

†Permanent address: Institut für Kern- und Teilchenphysik, Technische Universität Dresden, D-01069 Dresden, Germany.

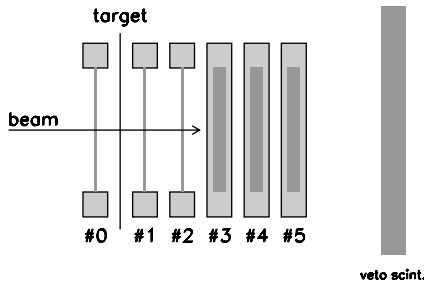


FIG. 1. Detector setup at the focal plane of the A1900 fragment separator for isotopic identification of reaction products using the  $\Delta E-E$  method. Diffraction-dissociation events where a light charged particle like a proton leaves the target can be discriminated against using the veto scintillation detector.

values for the thicknesses, since the range curve is not matched to them. By construction, thickness spectra give isotopic identification independent of kinetic energy. The third mass indicator relies on the parametrization  $R(E) \propto E^\alpha$  of the range curve [10] from which the following mass indicator is derived:

$$\ln(\alpha \Delta E) + (\alpha - 1) \ln(E + c \Delta E) - \alpha \ln(300), \quad (3)$$

where  $\alpha = a - b \Delta E/T$  and  $T$  is the  $\Delta E$ -detector thickness in micrometer. With this mass indicator, we use Si detector #4 and #5 as  $\Delta E$  and  $E$  detector, respectively. With calibration of the parameters  $a$ ,  $b$ , and  $c$  within their proper ranges, all three mass indicators give very similar results.

Figure 2 shows the mass-indicator spectra for reaction products from proton stripping using a  $^{27}\text{F}$  and  $^{29}\text{Ne}$  beam, respectively. For fluorine reaction products from the  $^{29}\text{Ne}$  beam, Eq. (1) gives the best result. For oxygen reaction products from the  $^{27}\text{F}$  beam, we use Eq. (3). Moreover, for the latter reaction, we require (i) no hits in the veto scintillator which discriminates against diffraction-dissociation events where the stripped protons exit the target and will deposit energy in the following Si detectors alongside the oxygen fragments, and (ii) an upper limit of  $\sim 850$  MeV for energy deposition in detector #4 in order to get rid of slow oxygen isotopes. The second condition is necessary since the calibration of the Si detectors and mass indicators is not well constrained for events where slow reaction products are almost stopped in detector #4, thus depositing most of their energy in there and very little in detector #5.

No events corresponding to  $^{26}\text{O}$  or  $^{28}\text{F}$  are visible in the mass-indicator spectra. The presence of lighter isotopes can be explained by either sequential neutron decay after proton-stripping events in which the residual nucleus is left in neutron-unbound states, or by more dissipative reactions like  $1p$ ,  $xn$ ,  $d$ , or  $t$  stripping. By inspection, we estimate the FWHM of the resolved mass peaks in the upper panel as  $\sim 3$  channels. We interpret the single count for the unbound  $^{25}\text{O}$  nucleus in the upper panel as belonging to the tail of the  $^{24}\text{O}$  mass peak. Assuming Gaussian shapes of the mass peaks with  $\sigma = \text{FWHM}/\sqrt{8 \ln 2} \approx 1.3$  channels, the chance to obtain events more than 2.5 channels higher than their centers is in the order of 2.5%. With ten counts falling squarely within the mass peak of  $^{24}\text{O}$ , we have to expect in average 0.25 counts more than 2.5 channels higher than its center due to  $^{24}\text{O}$  events.

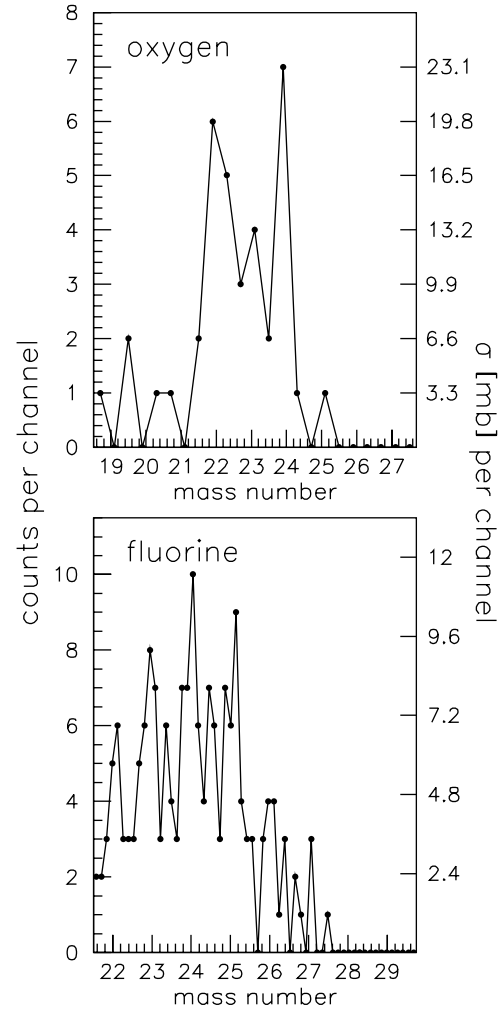


FIG. 2. Mass-indicator spectra for reaction products from proton stripping using a  $^{27}\text{F}$  (upper panel) and  $^{29}\text{Ne}$  (lower panel) beam.

Thus, the observed single count for  $^{25}\text{O}$  does not necessarily indicate that  $^{25}\text{O}$  is a particle-bound nucleus. In the case of  $^{26}\text{O}$ , since we are now about 4.5 channels higher than the center of the  $^{24}\text{O}$  mass peak, we would expect only  $\sim 2 \times 10^{-3}$  counts for every ten counts in the  $^{24}\text{O}$  mass peak. Therefore, around  $^{26}\text{O}$ , the mass-indicator spectrum is virtually background free.

Given target thickness and the total number of incoming beam particles, each count in the fluorine mass-indicator spectrum equates a production cross section of  $\sim 1.2$  mb, assuming 100% detection efficiency. Thus, the nonobservation of  $^{28}\text{F}$  corresponds to an upper limit of its production cross section by proton stripping from  $^{29}\text{Ne}$  of  $\sim 1.2$  mb. Production cross sections of lower-mass fluorine isotopes (involving the removal of neutrons) are in the order of 15–40 mb, in good agreement with earlier measurements in this mass region [9]. The exact numbers should actually be reduced somewhat to account for reactions which occurred in the last layers of detector #0 or the first layers of detector #1.

The production cross sections include events where the proton remains stuck in the target (knockout) and where it exits the target with roughly the same speed as the fragment

(diffraction dissociation). In the latter case, the protons will induce signals in the veto scintillator. For the production of fluorine isotopes,  $\sim 40\%$  of all events show coincident hits in the scintillator. Assuming that all of these events are related to diffraction-dissociation processes while all events without scintillator response are related to knockout processes, the total production cross section for each fluorine isotope will split up roughly as 40 and 60% between the two processes.

In the case of oxygen isotopes, since we require no hits in the veto scintillator, diffraction-dissociation processes are excluded from the data. Assuming the same ratio between knockout and diffraction-dissociation events as for the production of fluorine isotopes, each count in the mass-indicator spectrum equates a production cross section of  $\sim 2.0$  mb for the knockout process alone, and of  $\sim 3.3$  mb for knockout and diffraction-dissociation processes combined. The nonobservation of  $^{26}\text{O}$  corresponds therefore to an upper limit of its production cross section by proton stripping from  $^{27}\text{F}$  of  $\sim 3.3$  mb which is only slightly less than the experimental value of  $3.8 \pm 0.6$  mb for the similar ( $^{25}\text{F}, ^{24}\text{O}$ ) proton-stripping cross section of Ref. [9]. We neglect here the effect of the cut on the maximum energy deposition in detector #4, since events which would be affected by this cut would correspond to a quite dissipative production mechanism of  $^{26}\text{O}$ . However, this cut might impact the detection efficiency of lighter oxygen isotopes considerably. Production cross sections of lighter oxygen isotopes (involving neutron removal) are in the order of  $\sim 30$  mb, where some uncertainty has to be attributed to

the energy cut in the spectrum of Si detector #4. Again, the production cross sections are very similar to the production cross sections of oxygen isotopes from proton stripping (with additional removal of one or more neutrons) of lighter fluorine beams which were measured to be  $\sim 10$  mb [9]. However, in the present work, production of oxygen isotopes due to proton stripping in the last layers of detector #0 and the first layers of detector #1 has been neglected. When taken into account, this effect reduces the quoted production cross sections somewhat.

In conclusion, we have investigated the proton-stripping reactions of  $^{27}\text{F}$  and  $^{29}\text{Ne}$ . No events of  $^{26}\text{O}$  or  $^{28}\text{F}$  have been observed which corresponds to upper limits of their production cross sections in the order of 3.3 mb and 1.2 mb, respectively, compared to earlier cross-section measurements of similar reactions on neighboring particle-bound isotopes in the order of 4–6 mb. Production cross sections of lighter isotopes (involving neutron removal) are in the order of 10–40 mb, comparable with earlier results from proton stripping of lighter fluorine beams in the order of  $\sim 10$  mb. From the relatively low upper limit for production of  $^{28}\text{F}$ , we conclude that this isotope is not particle bound. In the case of  $^{26}\text{O}$ , our upper limit is not statistically significant, thus, our experiment cannot answer the question whether  $^{26}\text{O}$  is particle bound as early calculations indicated, or whether it is unbound, in agreement with more recent theoretical results using a modified shell-model interaction.

This work was supported by the National Science Foundation Grant No. PHY01-10253.

- 
- [1] M. Fauerbach, D. J. Morrissey, W. Benenson, B. A. Brown, M. Hellström, J. H. Kelley, R. A. Kryger, R. Pfaff, C. F. Powell, and B. M. Sherrill, *Phys. Rev. C* **53**, 647 (1996).
- [2] H. Sakurai *et al.*, *Phys. Lett.* **B448**, 180 (1999).
- [3] B. A. Brown, *Prog. Part. Nucl. Phys.* **47**, 517 (2001).
- [4] T. Otsuka, R. Fujimoto, Y. Utsuno, B. A. Brown, M. Honma, and T. Mizusaki, *Phys. Rev. Lett.* **87**, 082502 (2001).
- [5] Y. Utsuno, T. Otsuka, T. Mizusaki, and M. Honma, *Phys. Rev. C* **64**, 011301(R) (2001).
- [6] A. Volya and V. Zelevinsky, *Phys. Rev. Lett.* **94**, 052501 (2005).
- [7] M. Langevin *et al.*, *Phys. Lett.* **B150**, 71 (1985).
- [8] F. Pougheon *et al.*, *Europhys. Lett.* **2**, 505 (1986).
- [9] M. Thoennessen *et al.*, *Phys. Rev. C* **68**, 044318 (2003).
- [10] T. Shimoda, M. Ishihara, K. Nagatani, and T. Nomura, *Nucl. Instrum. Methods Phys. Res.* **165**, 261 (1979).